PROCEEDINGS OF SPIE

SPIEDigitalLibrary.org/conference-proceedings-of-spie

Multidimensional tomography of an entangled photon-pair source using stimulated emission

Bin Fang, Offir Cohen, Marco Liscidini, John E. Sipe, Virginia O. Lorenz

Bin Fang, Offir Cohen, Marco Liscidini, John E. Sipe, Virginia O. Lorenz, "Multidimensional tomography of an entangled photon-pair source using stimulated emission," Proc. SPIE 10118, Advances in Photonics of Quantum Computing, Memory, and Communication X, 101180G (20 February 2017); doi: 10.1117/12.2250349

SPIE.

Event: SPIE OPTO, 2017, San Francisco, California, United States

Invited Paper

Multidimensional tomography of an entangled photon-pair source using stimulated emission

Bin Fang[a], Offir Cohen[b], Marco Liscidini[c], John E. Sipe[d], and Virginia O. Lorenz[a]

[a]University of Illinois at Urbana-Champaign, Urbana, IL, USA
[b]Joint Quantum Institute, National Institute of Standards and Technology & University of Maryland, Gaithersburg, MD, USA; currently unaffiliated
[c]Department of Physics, University of Pavia,Via Bassi 6, I-27100 Pavia, Italy
[d]Institute for Optical Sciences, University of Toronto, 60 St. George Street, Ontario M5S 1A7, Canada

ABSTRACT

We demonstrate characterization of the joint spectral density of photon pairs and the energy-resolved reconstruction of the polarization density matrix of entangled photon pairs using stimulated emission tomography. The stimulated photons can be detected with high signal-to-noise ratio, allowing the efficient, high-resolution measurement of correlations within and between degrees of freedom. Stimulated emission tomography can thus be used for swift multidimensional characterization of photonic quantum information processing systems.

Keywords: Quantum Optics; Quantum information and processing; Nonlinear optics, fibers

Photonic quantum states are the foundation of protocols for quantum communication[1] and quantum applications in computing[2] and metrology.[3] Performing appropriate measurements to characterize sources of photonic quantum states[4–8] and tailoring them to be suitable for quantum applications[9] are topics of great current interest. A standard characterization technique is quantum state tomography (QST),[10] which requires a series of coincidence-counting-based projective measurements in the parameters of interest to reconstruct the density matrix of the quantum state. For sources based on spontaneous processes, such as spontaneous parametric down-conversion[11] or spontaneous four-wave mixing,[12] the low generation rates and detection efficiencies combined with background or accidental coincidence counts make it challenging to achieve high signal-to-noise ratio measurements, particularly when attempting to measure correlations across multiple degrees of freedom. Thus, while multidimensional quantum state tomography has been achieved for certain cases,[13,14] using QST for high-resolution characterization in arbitrary subspaces remains a challenge. To address this issue the technique of stimulated emission tomography (SET)[15] was recently proposed, which employs the stimulated version of the photon-pair generation process to enhance the measured signal by many orders of magnitude. The signal can thus be measured efficiently without the need for single-photon-level sensitivity and with high resolution. This technique has been applied to the characterization of photon-pair joint spectra,[16,17] polarization entanglement,[18] and multidimensional tomography in the polarization and frequency degrees of freedom.[19] Here we discuss our applications of the technique to characterize an optical-fiber-based source of photon pairs by measuring the joint spectral density[17] and performing a multidimensional tomography of polarization-entangled photon pairs.[19]

We generate photon pairs in birefringent optical fiber via spontaneous four-wave mixing[20] (see Fig. 1), in which two pump photons at frequency ω_p and polarization σ_p are annihilated and signal and idler photons at frequencies ω_s and ω_i and polarizations σ_s and σ_i, respectively, are created. Energy conservation dictates $\omega_s+\omega_i=2\omega_p$ and birefringent phase-matching results in the momentum conservation condition $\Delta k = 2k(\omega_p) - k(\omega_s) - k(\omega_i) + \Delta n\omega_p/c = 0$, where c is the speed of light and Δn is the difference in index of refraction between the slow axis, along which the pump propagates, and the fast axis, along which the signal and idler photons are generated. The generated photon-pair state can be represented as

$$|\Psi\rangle = \sum_{\sigma_s,\sigma_i} \iint d\omega_s d\omega_i \psi_{\sigma_s\sigma_i}(\omega_s,\omega_i)|\sigma_s\omega_s\rangle|\sigma_i\omega_i\rangle \tag{1}$$

Further author information: (Send correspondence to V. O. Lorenz)
V.O.L.: E-mail: vlorenz@illinois.edu, Telephone: 1 217 300 3306

Advances in Photonics of Quantum Computing, Memory, and Communication X, edited by Zameer Ul Hasan, Philip R. Hemmer, Hwang Lee, Alan L. Migdall, Proc. of SPIE Vol. 10118, 101180G
 · doi: 10.1117/12.2250349

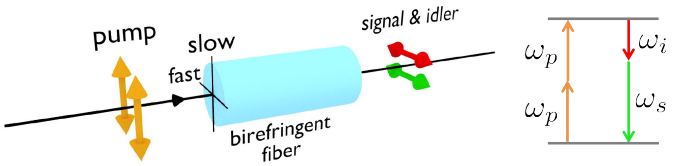

Figure 1. Schematic of photon-pair generation in polarization-maintaining optical fiber and energy diagram for the interaction. Two pump photons with frequency ω_p and polarization along the slow axis of the fiber are spontaneously annihilated in the $\chi^{(3)}$ material and signal and idler photons are created with frequency ω_s and ω_i, respectively, and polarization on the fast axis of the fiber. The photons obey energy conservation as indicated by the energy level diagram on the right.

where we have traced over the spatial degree of freedom because our source is single-mode fiber, and the biphoton wavefunction $\psi_{\sigma_s\sigma_i}(\omega_s, \omega_i)$ is resolved in both the polarization and frequency degrees of freedom. If no correlations between degrees of freedom exist, the wavefunction can be separated into two functions that each depend on one degree of freedom:

$$|\Psi\rangle_{\text{sep}} = |\Phi\rangle_{\omega_s,\omega_i} \otimes |\Sigma\rangle_{\sigma_s,\sigma_i}, \tag{2}$$

where $|\Phi\rangle_{\omega_s,\omega_i}$ depends solely on the joint spectrum $f(\omega_s, \omega_i)$:

$$|\Phi\rangle_{\omega_s,\omega_i} = \iint d\omega_s d\omega_i f(\omega_s, \omega_i)|\omega_s\rangle|\omega_i\rangle, \tag{3}$$

and $|\Sigma\rangle_{\sigma_s,\sigma_i}$ represents the joint polarization state. However, if correlations do exist between frequency and polarization, the wave function is not separable, and a multidimensional tomography is required. For example, to perform an energy-resolved polarization-state tomography, measurements in frequency ranges $\delta\omega_s\delta\omega_i$ for which correlations are negligible would be taken across the bandwidths of the generated photons, rather than collecting across all frequencies, as is commonly done in QST with broadband single photon detectors.[21]

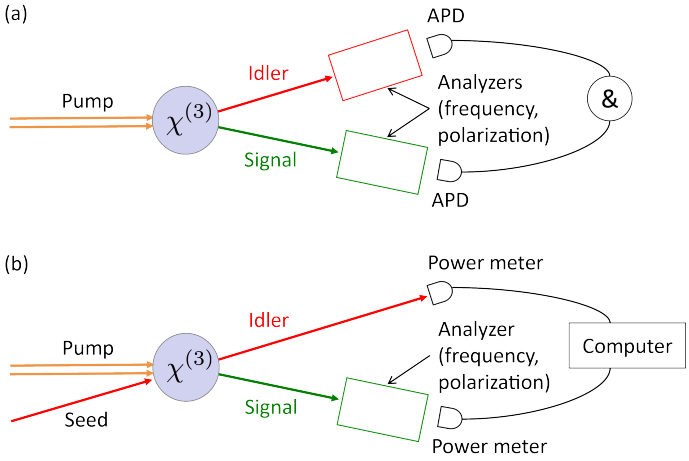

Figure 2. (a) Schematic of quantum state tomography. The source of photonic quantum states is characterized by projecting the emitted photons onto a series of basis states in the degrees of freedom of interest and counting coincidences. (b) Schematic of stimulated emission tomography. A seed laser prepared in a series of basis states stimulates the signal. The amplified signal is proportional to the signal photons generated in the spontaneous process and can be measured without the need for single-photon-level sensitivity.

The difference between quantum state tomography and stimulated emission tomography is shown schematically in Fig. 2. In QST, the emitted photons are projected onto basis states in the degrees of freedom of interest, and single-photon detectors are used to count coincidences for each basis state. To measure the joint spectral density, for example, the signal and idler photons would be sent to monochromators and coincidences

would be counted for each frequency pair.[20] The low generation rate of the source combined with tight spectral filtering results in poor signal-to-noise ratio and low resolution. To perform an energy-resolved polarization-state tomography of, for example, a polarization-entangled photon-pair source with energy-polarization correlations, many such spectrally resolved measurements with bandwidths $\delta\omega_s\delta\omega_i$ across which correlations are negligible would be required, resulting in prohibitively long acquisition times. In SET, a laser is used to seed one of the photons, in this case the idler, such that the seeded state matches the basis state in which one wishes to measure; the stimulated signal is then proportional to the coincidence measurement, but amplified by many orders of magnitude:[15]

$$\langle n_{\sigma_s\omega_s}\rangle_{A_{\sigma_i\omega_i}} \approx \langle n_{\sigma_s\omega_s} n_{\sigma_i\omega_i}\rangle \times |A_{\sigma_i\omega_i}|^2, \tag{4}$$

where $\langle n_{\sigma_s\omega_s}\rangle_{A_{\sigma_i\omega_i}}$ is the average number of stimulated signal photons, $\langle n_{\sigma_s\omega_s} n_{\sigma_i\omega_i}\rangle$ is the average number of photon pairs that are spontaneously generated, and $|A_{\sigma_i\omega_i}|^2$ is the average photon number within the coherence time of the seed. For joint spectral density measurements, the stimulated signal can be measured with a spectrometer as the seed laser is scanned across the bandwidth of the idler. The amplified signal can thus be measured with high signal-to-noise ratio and high resolution, without the need for single photon detection. The improved acquisition times compared to QST allow for efficient measurement of the joint spectral density and energy-resolved polarization state tomography. In optical fiber the primary source of background photons is Raman scattering; here the birefringent phase-matching condition results in idler photons far detuned from the pump and thus the Raman background is relatively small.[20] Note that the seed will not stimulate at the signal wavelength via Raman scattering. Thus, in general, noise processes not stimulated by the seed must be characterized at the single-photon level.

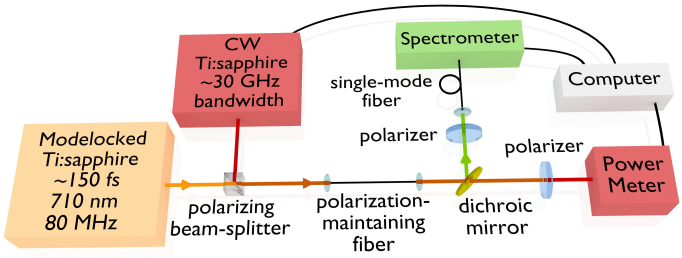

Figure 3. Experimental setup for measurement of the joint spectral density. The pump and seed lasers interact with the optical fiber to generate stimulated signal photons. The signal and idler photons are separated by a dichroic mirror. The seed idler photons are detected by a power meter to normalize out any intensity variations of the seed. The stimulated signal photons are frequency-resolved with a spectrometer.

In order to measure the joint spectral density $|f(\omega_s,\omega_i)|^2$ using stimulated emission tomography, we use a continuous-wave (CW) Ti:sapph laser with ~ 30 GHz bandwidth to seed the idler photons generated by a modelocked Ti:sapph laser in polarization-maintaining optical fiber (see Fig. 3). We use a polarizer to eliminate the pump light from the photons, which also ensures the photons can be represented by the product of a single joint polarization state and the wavefunction dependent on the joint spectrum shown in Eq. 3. The stimulated signal photons are frequency-resolved using a spectrometer with 0.06 nm resolution. We collect signal spectra for a series of idler wavelengths across the bandwidth of the spontaneously generated idler photons with a resolution of 0.1 nm. A typical joint spectral density measurement is shown in Fig. 4(a). The full data acquisition takes approximately 10 minutes and is limited by the mechanical adjustment of the seed laser frequency. To perform a similar measurement using QST requires many hours, limited by coincidence count rate, and results in much lower signal-to-noise ratio.

For comparison with the theoretically expected joint spectral density, we calculate the joint spectral density following a standard approach[22] in which we determine the Hamiltonian for the four-wave mixing interaction and compute the evolution of the pump state. The joint spectral density can be written as:[20]

$$|f(\omega_s,\omega_i)|^2 = \left|\int \mathrm{d}\omega_p \alpha(\omega_p)\alpha(\omega_s+\omega_i-\omega_p)\phi(\omega_s,\omega_i)\right|^2, \tag{5}$$

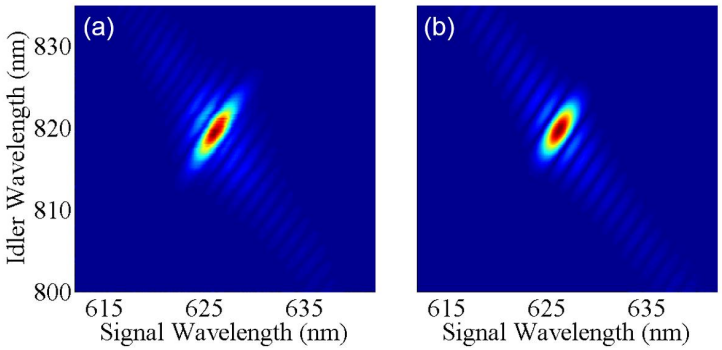

Figure 4. (a) Experimental result of the joint spectral density, showing high signal-to-noise ratio and clear sidelobes. (b) Theoretical result, indicating good agreement with experiment.

where $\alpha(\omega_p)$ is the pump envelope function and is assumed to take a Gaussian form, and

$$\phi(\omega_s, \omega_i) = \text{sinc}\left(\frac{\Delta kL}{2}\right) \exp\left(\frac{i\Delta kL}{2}\right) \tag{6}$$

is the phase-matching function, where L is the length of the fiber and

$$\Delta k = 2n(\omega_p)\omega_p/c - n(\omega_s)\omega_s/c - n(\omega_i)\omega_i/c + \Delta n\omega_p/c \tag{7}$$

is the phase mismatch, with $n(\omega)$ the refractive index given by the Sellmeier equation of bulk silica, Δn the birefringence of the fiber and c the speed of light in free space. The experimental results have 93% fidelity with the calculated joint spectral density, shown in Fig. 4(b). The experimental data have high enough signal-to-noise ratio to clearly show the presence of side lobes, which arise from the sudden turning on and turning off of the four-wave-mixing interaction as the pump enters and leaves the fiber.[23]

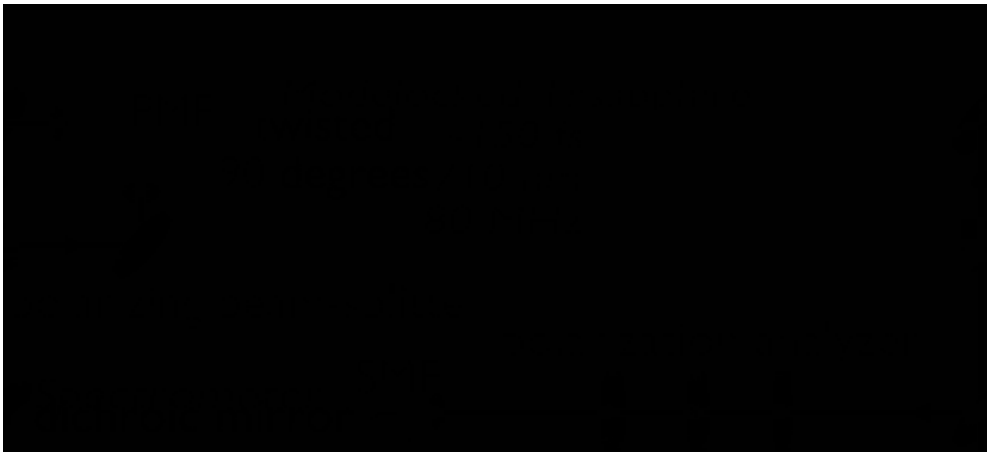

Figure 5. Schematic of the experimental setup for frequency-resolved stimulated emission tomography of polarization-entangled photon pairs generated in optical fiber. The polarization-entangled photon pairs are generated in a Sagnac loop geometry. A CW seed laser is prepared in a series of polarization basis states and frequencies before being launched into the Sagnac loop where it stimulates the signal photons. The idler photons are detected with a power meter to normalize out intensity variations and the signal photons are sent to a polarization analyzer that projects them into various basis states and a spectrometer that records their spectrum.

To demonstrate SET's multidimensional tomography capability, we perform a frequency-resolved polarization state tomography of polarization-entangled photon pairs emitted from optical fiber in a Sagnac loop.[24] In this case, we project the photons onto a series of joint polarization basis states, each of which may exhibit dependence

on the joint frequency of the photon pairs. Thus, the biphoton wavefunction may not be represented as in Eq. 2. In order to measure the state without averaging over frequency, we perform the tomography for a series of joint frequency ranges $\delta\omega_s\delta\omega_i$ over which the correlations are negligible. We then reconstruct the frequency-resolved polarization density matrix of the photon-pair state. As shown in Fig. 5, a modelocked Ti:sapph laser centered at 715 nm with 150 fs pulses is sent into the Sagnac loop, with 5 mW of horizontally (vertically) polarized light propagating counter-clockwise (clockwise) through the 20 cm-long polarization-maintaining fiber. We set the target polarization state at the output of the loop to be $(|H_sH_i\rangle + |V_sV_i\rangle)/\sqrt{2}$; however, the actual polarization-entangled photon-pair state may be frequency-correlated. A CW Ti:sapph seed laser with a power of 10 mW and $\sim$ 30 GHz bandwidth is sent through both ports of the loop, stimulating the signal photons for a series of idler frequencies and idler polarization states. The power of the seed laser is recorded in order to normalize out any variations in power during the measurement.

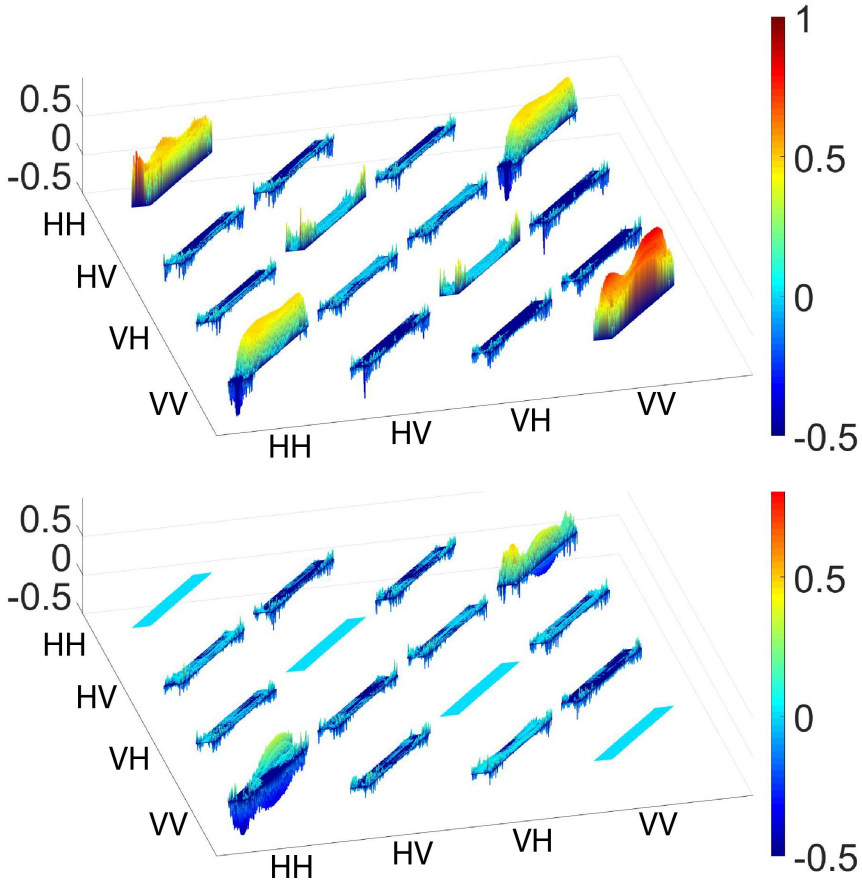

Figure 6. Real (top) and imaginary (bottom) parts of the frequency-resolved density matrix obtained using SET. Each matrix element is comprised of 4600 elements corresponding individual frequency pairs, with the x-axis corresponding to the wavelength of the signal and the y-axis to that of the idler. The spectral footprint corresponds to shape of the joint spectrum of the photon pairs.

The resulting three-dimensional SET data is composed of 4600 individual density matrices measured with frequency bandwidths $\delta\omega_s\delta\omega_i \sim 0.6\,\text{nm} \times 0.1\,\text{nm}$, shown in Fig. 6. To analyze the properties of the entangled state represented by the frequency-resolved density matrix, we calculate the tangles, fidelities to the target state $|H_sH_i\rangle + |V_sV_i\rangle$ and purities for all frequency pairs, shown in Fig. 7. These properties provide useful and detailed information with which to characterize the source that can not be easily obtained from quantum state tomography. As can be seen from the plot of the tangle in Fig. 7(a), most of the tangles are high and the peak tangle is approximately 0.99. However, the overall tangle is 0.80. There are several factors that may contribute

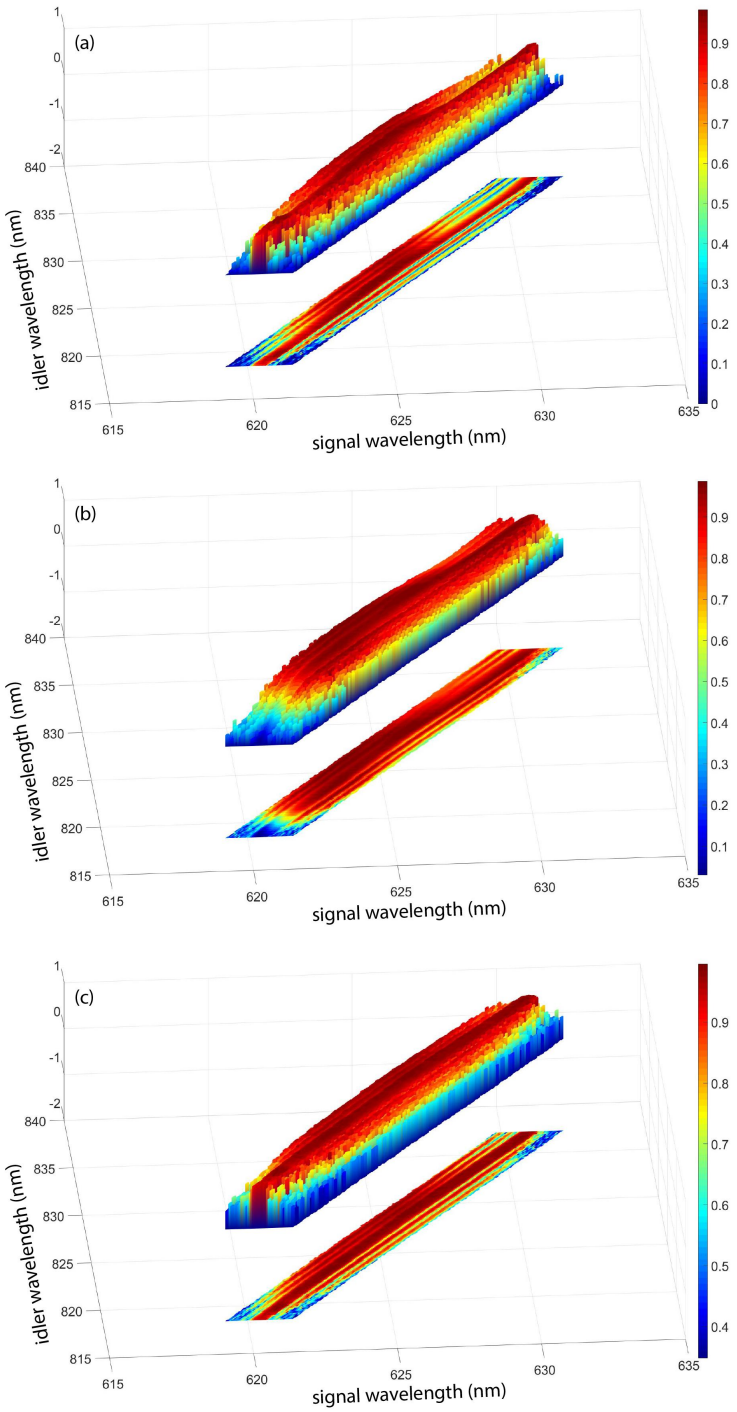

Figure 7. (a) The frequency-resolved tangle, (b) fidelity to the target state $|H_s H_i\rangle + |V_s V_i\rangle$ and (c) purity of the photon-pair state measured by frequency-resolved SET in the optical-fiber-based polarization-entangled photon pair source. The detailed structure revealed in these plots can be used to diagnose and control correlations within and between the energy and polarization degrees of freedom.

to this deterioration of the quality of the source. The photons generated by the wings of the pump pulse may be more sensitive to the presence of noise; although these photons have much lower count rates, applying a broadband spectral filter that filters out the photons in the wings ($\sim 10\%$ of the total photons) increases the tangle by approximately 10%. The fidelity in Fig. 7(b) may additionally be influenced from variations in the balance of amplitudes between the two pathways and the presence of frequency-dependent birefringence in the polarization-maintaining fiber and other optics that results in variations of the joint phase across the photon-pair joint spectrum. The plot of purity in Fig. 7(c) indicates the majority of photon pairs can be represented by a pure state, even pairs that have obviously low tangle. These properties of tangle, fidelity and purity together suggest nearly perfect entanglement can be achieved using tight spectral filtering, which is often done in photon-pair source demonstrations.[25]

In conclusion, we have shown that stimulation emission tomography enables efficient, highly resolved multi-dimensional characterization of sources of photonic quantum states. By applying SET to our optical-fiber-based source we are able to swiftly measure the joint spectral density and reconstruct an energy-resolved polarization density matrix that would be prohibitive to obtain via QST. This technique can be extended to other quantum information processing systems to characterize and engineer the output photonic quantum state.

This work was supported in part by the NSF Physics Division, Grant Nos. 1205812 and 1521110 and the Natural Sciences and Engineering Research Council of Canada.

REFERENCES

[1] Gisin, N. and Thew, R., "Quantum communication," *Nat. Photon.* **1**(3), 165–171 (2007).
[2] Knill, E., Laflamme, R., and Milburn, G. J., "A scheme for efficient quantum computation with linear optics," *Nature* **409**(6816), 46–52 (2001).
[3] Nagata, T., Okamoto, R., O'Brien, J. L., Sasaki, K., and Takeuchi, S., "Beating the Standard Quantum Limit with Four-Entangled Photons," *Science* **316**(5825), 726–729 (2007).
[4] Avenhaus, M., Eckstein, A., Mosley, P. J., and Silberhorn, C., "Fiber-assisted single-photon spectrograph," *Opt. Lett.* **34**(18), 2873–2875 (2009).
[5] Hariharan, P., [*Optical Interferometry*], Academic Press, San Diego & London (2003).
[6] Wasilewski, W., Wasylczyk, P., Kolenderski, P., Banaszek, K., and Radzewicz, C., "Joint spectrum of photon pairs measured by coincidence Fourier spectroscopy," *Opt. Lett.* **31**(8), 1130–1132 (2006).
[7] Christ, A., Laiho, K., Eckstein, A., Cassemiro, K. N., and Silberhorn, C., "Probing multimode squeezing with correlation functions," *New J. Phys.* **13**(3), 033027 (2011).
[8] Hanbury Brown, R. and Twiss, R. Q., "Correlation between Photons in two Coherent Beams of Light," *Nature* **177**(4497), 27–29 (1956).
[9] Cohen, O., Lundeen, J. S., Smith, B. J., Puentes, G., Mosley, P. J., and Walmsley, I. A., "Tailored Photon-Pair Generation in Optical Fibers," *Phys. Rev. Lett.* **102**(12), 123603 (2009).
[10] James, D. F. V., Kwiat, P. G., Munro, W. J., and White, A. G., "Measurement of qubits," *Phys. Rev. A* **64**(5), 052312 (2001).
[11] Kwiat, P. G., Mattle, K., Weinfurter, H., Zeilinger, A., Sergienko, A. V., and Shih, Y., "New High-Intensity Source of Polarization-Entangled Photon Pairs," *Phys. Rev. Lett.* **75**(24), 4337–4341 (1995).
[12] Li, X., Voss, P. L., Sharping, J. E., and Kumar, P., "Optical-Fiber Source of Polarization-Entangled Photons in the 1550 nm Telecom Band," *Phys. Rev. Lett.* **94**(5), 053601 (2005).
[13] Barreiro, J. T., Langford, N. K., Peters, N. A., and Kwiat, P. G., "Generation of Hyperentangled Photon Pairs," *Phys. Rev. Lett.* **95**(26), 260501 (2005).
[14] Beck, M., "Quantum State Tomography with Array Detectors," *Phys. Rev. Lett.* **84**(25), 5748–5751 (2000).
[15] Liscidini, M. and Sipe, J. E., "Stimulated Emission Tomography," *Phys. Rev. Lett.* **111**(19), 193602 (2013).
[16] Eckstein, A., Boucher, G., Lematre, A., Filloux, P., Favero, I., Leo, G., Sipe, J. E., Liscidini, M., and Ducci, S., "High-resolution spectral characterization of two photon states via classical measurements," *Laser & Photonics Reviews* **8**, L76–L80 (2014).
[17] Fang, B., Cohen, O., Liscidini, M., Sipe, J. E., and Lorenz, V. O., "Fast and highly resolved capture of the joint spectral density of photon pairs," *Optica* **1**(5), 281–284 (2014).

[18] Rozema, L. A., Wang, C., Mahler, D. H., Hayat, A., Steinberg, A. M., Sipe, J. E., and Liscidini, M., "Characterizing an entangled-photon source with classical detectors and measurements," *Optica* **2**(5), 430–433 (2015).

[19] Fang, B., Liscidini, M., Sipe, J. E., and Lorenz, V. O., "Multidimensional characterization of an entangled photon-pair source via stimulated emission tomography," *Opt. Express* **24**(9), 10013–10019 (2016).

[20] Smith, B. J., Mahou, P., Cohen, O., Lundeen, J. S., and Walmsley, I. A., "Photon pair generation in birefringent optical fibers," *Opt. Express* **17**(26), 23589–23602 (2009).

[21] Kwiat, P. G., Steinberg, A. M., Chiao, R. Y., Eberhard, P. H., and Petroff, M. D., "High-efficiency single-photon detectors," *Phys. Rev. A* **48**(2), R867–R870 (1993).

[22] Chen, J., Li, X., and Kumar, P., "Two-photon-state generation via four-wave mixing in optical fibers," *Phys. Rev. A* **72**(3), 033801 (2005).

[23] Fang, B., Cohen, O., Moreno, J. B., and Lorenz, V. O., "State engineering of photon pairs produced through dual-pump spontaneous four-wave mixing," *Opt. Express* **21**(3), 2707–2717 (2013).

[24] Fang, B., Cohen, O., and Lorenz, V. O., "Polarization-entangled photon-pair generation in commercial-grade polarization-maintaining fiber," *J. Opt. Soc. Am. B* **31**(2), 277–281 (2014).

[25] Grice, W. P., Erdmann, R., Walmsley, I. A., and Branning, D., "Spectral distinguishability in ultrafast parametric down-conversion," *Phys. Rev. A* **57**(4), R2289–R2292 (1998).